RSC Advances

PAPER

View Article Online
View Journal | View Issue

Cite this: *RSC Adv.*, 2025, **15**, 29424

Cu/ZnO@GO promoted green synthesis of novel dipyridopyrimidines: evaluation of biological activity and theoretical study of the mechanism using a DFT method

Elham Ezzatzadeh, *[a] Nasrin Karami Hezarcheshmeh[b] and Reza Akbari[c]

This investigation presents a single-step reaction performed at ambient temperature in aqueous media, involving acetylacetone, aldehydes, guanidine, and activated acetylenic compounds, employing a catalytic system consisting of small quantities of Cu/ZnO@GO. Currently, the antioxidant potential of select synthesized dipyridopyrimidines is evaluated *via* diphenyl-picrylhydrazine (DPPH) radical scavenging assays. Furthermore, the antimicrobial efficacy of the synthesized compounds was systematically assessed using the disk diffusion method, which involved testing against two distinct strains of Gram-negative bacteria and Gram-positive bacteria. In a separate vein, the catalytic efficacy of the Cu/ZnO@GO catalyst was rigorously assessed in the reduction of organic pollutants, specifically 4-nitrophenol (4-NP), in aqueous solutions under benign conditions. The data revealed that nanocomposites prepared *via* a biosynthetic method demonstrated remarkable catalytic performance in the remediation of organic contaminants, achieving substantial reduction within mere seconds. The synthetic methodology employed for the generation of dipyridopyrimidines was characterized by a confluence of advantageous attributes, encompassing accelerated reaction kinetics, elevated product yields, and facile recovery of the catalyst from the reaction milieu. Density Functional Theory (DFT) calculations at the B3LYP/6-311G(d,p) level were conducted to explore the reaction mechanism, employing the total energy of reactants and products as a basis for its determination.

Received 9th June 2025
Accepted 13th August 2025

DOI: 10.1039/d5ra04054j

rsc.li/rsc-advances

1. Introduction

Multicomponent reactions (MCRs) are a prevalent methodology for the synthesis of biologically active compounds.[1–5] In the context of heterocyclic compound production, MCRs demonstrate superior efficacy compared to alternative methodologies, esteemed as they are for their efficient yields and atom economy.[6–8] These heterocycles, readily sourced from natural origins and fundamentally important to biological processes, are found as structural components in a plethora of naturally occurring materials, including vitamins, hormones, and antibiotics. Consequently, the development of effective strategies for their synthesis is an area of considerable interest within the field of synthetic organic chemistry.[9] Nitrogen-containing heterocyclic compounds, particularly, are of considerable value in medicinal chemistry, exerting a beneficial influence across numerous facets of daily life. Given their diverse biological functionalities and significant roles in medicinal applications, heterocyclic compounds are recognized as exceptionally important organic molecules,[10–21] resulting in the establishment of myriad synthetic approaches to their formation.[22–25] Pyridopyrimidine derivatives, specifically, have garnered substantial attention due to their wide-ranging biological activities, encompassing anticancer,[26] antiviral,[27] anti-allergic,[28] anti-HIV,[29] and anti-inflammatory[30] properties. Catalysts are indispensable in certain manufacturing protocols for heterocyclic compounds. Graphene oxide (GO), acknowledged for its desirable characteristics such as a high surface area and notable adsorption capacity,[31–33] has been extensively investigated. Nanostructured transition metal oxides, possessing elevated active surface areas, can function as catalysts in these synthetic pathways. Beyond their fundamental scientific applications, these catalytic agents find extensive employment in both technological advancements and applied research endeavors. Of late, metal oxides and supported catalysts have garnered considerable interest, largely attributable to their remarkable selectivity and efficiency in promoting organic transformations. The distinctive catalytic efficacy and inherent crystalline organization characteristic of metal oxides set them apart within this domain.[34–37] This underscores the capacity to

[a]*Department of Chemistry, Ard.C., Islamic Azad University, Ardabil, Iran. E-mail: Elham.Ezzatzadeh@iau.ac.ir; dr.ezzatzadeh@yahoo.com*

[b]*Department of Chemistry, SR.C., Islamic Azad University, Tehran, Iran*

[c]*Department of Chemistry, Faculty of Basic Sciences, Gonbad Kavous University, Gonbad Kavous, Iran*

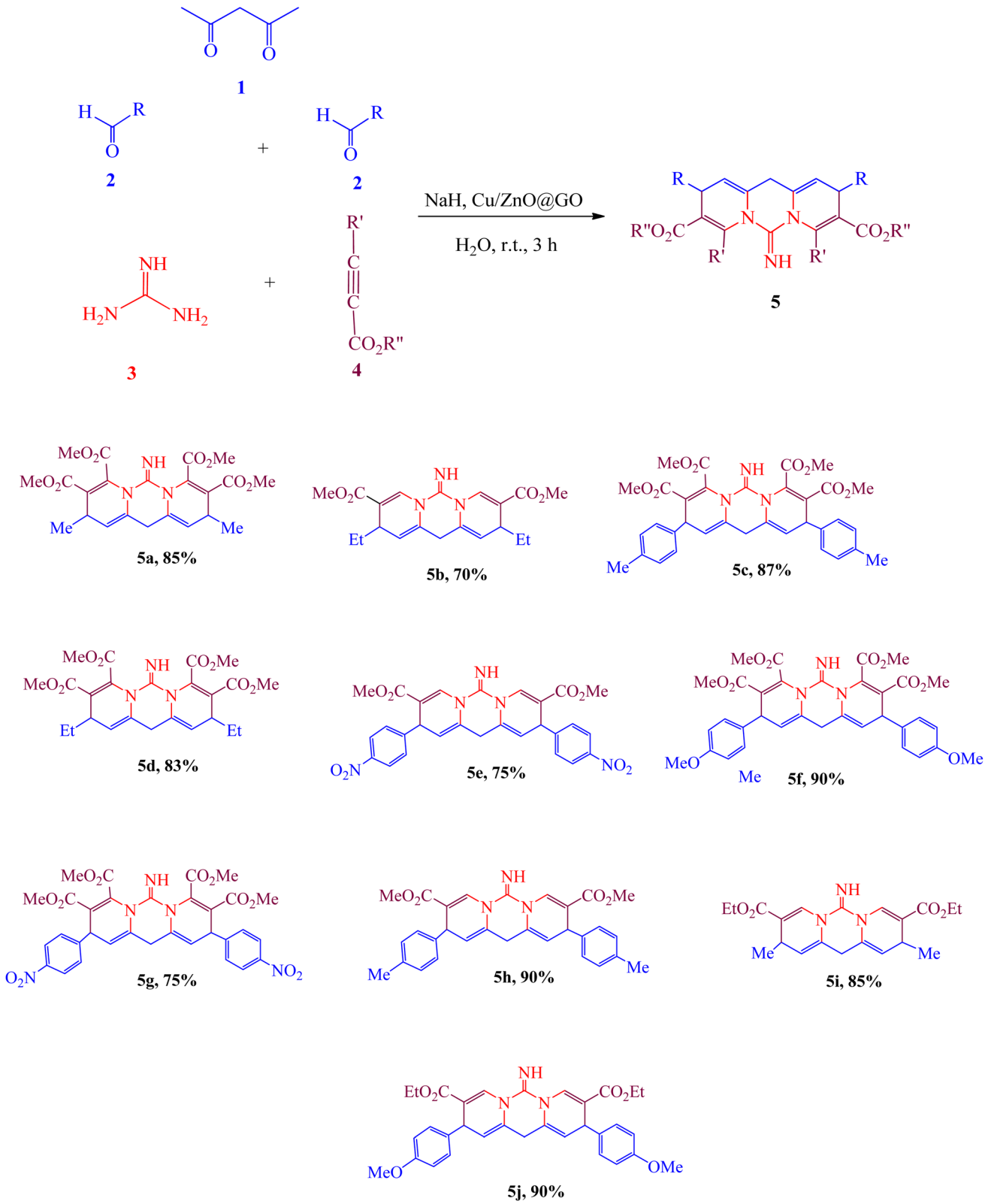

Scheme 1 Synthesis of dipyridopyrimidines 5.

tailor a material's surface characteristics to achieve optimal suitability for particular applications through strategic combination of multiple metallic elements and judicious implementation of diverse processing methodologies.[38–40] The incorporation of metal oxide catalysts within nanocomposite architectures has demonstrated remarkable effectiveness in the

green synthesis of heterocyclic compounds, adhering to principles of environmental sustainability. Such organic compounds frequently exhibit antioxidant capabilities stemming from chemical configurations that facilitate the mitigation of deleterious effects, thereby counteracting the detrimental influence of free radicals.[41–43] Furthermore, organic compounds possessing antioxidant attributes may contribute to the prevention or amelioration of specific disease states.[44–51] Investigation into the antibacterial characteristics of synthetically derived materials constitutes another critical area of inquiry pertaining to their broader biological functionalities. Diverse bacterial strains give rise to a spectrum of diseases impacting both human and animal populations, a subset of which prove refractory to existing treatment modalities. Consequently, synthesized compounds may exhibit the dual benefit of antioxidant and antimicrobial activity. Dyes and pigments, finally, find widespread application across a multitude of industrial sectors, encompassing textiles, cosmetics, printing, pharmaceuticals, and food processing. Approximately 700 000 tons of dyes and pigments are produced annually, most of which are harmful to aquatic life. As a result, it is necessary to enhance environmentally friendly and green methods for eliminating these harmful substances from our surroundings, owing to their toxic and cancer-causing characteristics. The literature describes various chemical and physical techniques for the behaviour of dyes, including their waste. However, some drawbacks of these approaches are the high costs, the creation of dangerous by-products, and the need for significant energy. Therefore, there is a need for more sustainable methods or chemical solutions to reduce or eliminate these issues. Recent studies have concentrated on finding new and straightforward techniques for creating important heterocyclic compounds.[52–80] This research uses an eco-friendly strategy to produce unique dipyridopyrimidines **5**. The process involves a reaction with multiple components using acetylacetone **1**, aldehydes **2**, guanidine **3**, and activated acetylenic compounds **4** in the presence of Cu/ZnO@GO as new efficient catalyst (Scheme 1).

2. Experimental section

2.1. General

The research team employed analytical reagents and solvents of exceptional purity, ensuring the stability of their physicochemical properties. To characterize the synthesized nanocatalysts and resultant dipyridopyrimidines, a Shimadzu IR-460 spectrometer was utilized. These analyses were conducted in a KBr matrix, with data acquisition performed *via* FT-IR spectroscopy. Furthermore, proton and carbon NMR spectra of the synthesized materials were acquired using a Bruker DRX-400 AVANCE spectrometer. This instrument was operated at a frequency of 400 MHz, employing $CDCl_3$ as the solvent and TMS as the internal standard for the spectra of the synthesized materials. The mass spectra of these compounds were recorded on a Finnigan MAT 8430 spectrometer, utilizing an ionization energy of 70 eV. Elemental analysis of the synthesized compounds was performed using a Heraeus CHN-O-Rapid analyzer. The successful fabrication of the synthetic catalyst Cu/ZnO@GO was corroborated through a suite of spectroscopic methods, including XRD, EDX, TEM and SEM.

2.2. Fabrication of Cu/ZnO@GO nanocatalyst

To prepare the solution, a precise amount of 1.5 grams of zinc acetate ($Zn(OAC)_2$) and 1.5 grams of $CuCl_2$ were individually dissolved in 5 mL of an aqueous extract derived from the rhizome of *Petasites hybridus*. This mixture was then heated together in a round-bottom flask until reaching a temperature of 200 °C, during which it was continuously stirred for one hour. Immediately following the completion of the reaction, it was crucial to rapidly cool the mixture to ambient temperature. Once cooled, the mixture was subjected to centrifugation at 7000 rpm for approximately ten minutes to remove any unreacted organic residues. The resulting Cu/ZnO nanoparticles were subsequently isolated, washed thoroughly with a solution comprising equal parts of ethanol and water, and then allowed to dry naturally at room temperature for 24 hours. To synthesize the nanocomposite, 0.1 grams of graphene oxide (GO) and 0.1 grams of Cu/ZnO nanoparticles were combined and mixed with 10 mL of the *Petasites hybridus* rhizome extract. This suspension was then subjected to vigorous agitation at 200 °C for one hour. The Cu/ZnO@GO nanocatalyst was then washed multiple times with a 50 : 50 ethanol–water solution to ensure purity. In conclusion, the targeted nanocomposite, Cu/ZnO@GO, was successfully synthesized with a high yield, demonstrating an efficient and reproducible approach.

2.3. Preparation procedure for dipyridopyrimidines 5a–5j

At ambient temperature, acetylacetone **1** (1 mmol), and aldehydes **2** (2 mmol) were mixed in the presence of sodium hydride (3 mmol) and catalyst (0.02 g) for 45 min. After this time guanidine **3** (1 mmol) was introduced into the mixture and stirred for 30 minutes. We stirred the fresh concoction for 45 minutes after including the activated acetylenic compound **4** (1 mmol) into the initial mixture following a lapse of 30 minutes. The reaction was completed within a three-hour timeframe, and thin-layer chromatography (TLC) was used to monitor the reaction progress. To produce pure title compounds **5**, a solid residue was isolated using filtering, subjected to cleaning with ethanol and diethyl ether, soluble in dichloromethane, and further purified using column chromatography with a 5 : 1 mixture of hexane and ethyl acetate.

2.3.1 Tetramethyl 6-imino-2,10-dimethyl-10,12-dihydro-2*H*,6*H*-dipyrido[1,2-*c*:2′,1′-*f*]pyrimidine-3,4,8,9-tetracarboxylate (5a). Yellow powder, m. p. 123–125 °C, yield: 85%. IR (KBr) (ν_{max}/cm^{-1}): 3347, 1742, 1735, 1587, 1487, 1385 and 1290 cm^{-1}. ^{1}H NMR (500 MHz, $CDCl_3$): δ_{ppm} 1.25 (6H, d, $^3J_{HH}$ = 7.2 Hz, $2CH_3$), 3.07 (1H, d, $^2J_{HH}$ = 6.5 Hz, CH), 3.18 (1H, d, $^2J_{HH}$ = 6.5 Hz, CH), 3.65 (6H, s, $2CH_3O$), 3.69 (2H, q, $^3J_{HH}$ = 7.2 Hz, 2CH), 3.75 (6H, s, $2CH_3O$), 5.86 (2H, s, 2CH), 9.44 (1H, s, NH). ^{13}C NMR (125.7 MHz, $CDCl_3$): δ_{ppm} 166.7, 165.5, 154.0, 145.3, 135.4, 121.2, 120.1, 53.0, 51.6, 32.1, 28.3, 21.4. MS, *m*/*z* (%): 459 (M^+, 10), 31 (100). Anal. calcd for $C_{22}H_{25}N_3O_8$ (459.16): C, 57.51; H, 5.48; N, 9.15; found: C, 57.63; H, 5.58; N, 9.28.

2.3.2 Dimethyl 2,10-diethyl-6-imino-10,12-dihydro-2*H*,6*H*-dipyrido[1,2-*c*:2′,1′-*f*]pyrimidine-3,9-dicarboxylate (5b). Yellow powder, m. p. 137–139 °C, yield: 70%. IR (KBr) (ν_{max}/cm^{-1}): 3357, 1738, 1732, 1575, 1475, 1385 and 1297. ^{1}H NMR (500 MHz, $CDCl_3$): δ_{ppm} 0.94 (6H, t, $^3J_{HH}$ = 6.8 Hz, 2CH$_3$), 1.59 (4H, m, 2CH$_2$), 3.06 (2H, s, CH$_2$), 3.43 (2H, t, $^3J_{HH}$ = 6.8 Hz, 2CH), 3.70 (6H, s, 2CH$_3$O), 5.74 (2H, s, 2CH), 8.24 (1H, s, 1CH), 8.67 (1H, s, NH). ^{13}C NMR (125.7 MHz, $CDCl_3$): δ_{ppm} 167.5, 151.7, 135.4, 134.3, 117.3, 109.4, 51.4, 46.7, 38.1, 27.9, 11.3. MS, *m*/*z* (%): 371 (M$^+$, 10), 31 (100). Anal. calcd for $C_{20}H_{25}N_3O_4$ (371.18): C, 64.67; H, 6.78; N, 11.31; found: C, 64.78; H, 6.86; N, 11.45%.

2.3.3 Tetramethyl 6-imino-2,10-di-*p*-tolyl-10,12-dihydro-2*H*,6*H*-dipyrido[1,2-*c*:2′,1′-*f*]pyrimidine-3,4,8,9-tetracarboxylate (5c). Yellow powder, m. p. 165–167 °C, yield: 87%. IR (KBr) (ν_{max}/cm^{-1}): 3448, 1745, 1738, 1556, 1478, 1385 and 1280. ^{1}H NMR (500 MHz, $CDCl_3$): δ_{ppm} 2.35 (6H, s, 2Me), 3.14 (1H, d, $^2J_{HH}$ = 6.5 Hz, CH), 3.22 (1H, d, $^2J_{HH}$ = 6.5 Hz, CH), 3.62 (6H, s, 2MeO), 3.74 (6H, s, 2MeO), 4.74 (2H, s, 2CH), 6.12 (2H, s, 2CH), 7.15 (4H, d, $^3J_{HH}$ = 7.6 Hz, 4CH), 7.17 (4H, d, $^3J_{HH}$ = 7.6 Hz, 4CH), 9.44 (1H, s, NH). ^{13}C NMR (125.7 MHz, $CDCl_3$): δ_{ppm} 165.9, 165.1, 154.1, 140.8, 140.7, 137.8, 137.1, 130.1, 128.3, 128.1, 115.7, 53.0, 51.6, 38.6, 32.2, 21.0. MS, *m*/*z* (%): 611 (M$^+$, 10), 31 (100). Anal. calcd for $C_{34}H_{33}N_3O_8$ (611.23): C, 66.77; H, 5.44; N, 6.87; found: C, 66.92; H, 5.62; N, 6.96%.

2.3.4 Tetramethyl 2,10-diethyl-6-imino-10,12-dihydro-2*H*,6*H*-dipyrido[1,2-*c*:2′,1′-*f*]pyrimidine-3,4,8,9-tetracarboxylate (5d). Yellow powder, m. p. 152–154 °C, yield: 83%. IR (KBr) (ν_{max}/cm^{-1}): 3435, 1742, 1738, 1465 and 1295. ^{1}H NMR (500 MHz, $CDCl_3$): δ_{ppm} 0.96 (6H, d, $^3J_{HH}$ = 6.8 Hz, 2CH$_3$), 1.67 (4H, m, 2CH$_2$), 3.10 (1H, d, $^2J_{HH}$ = 6.5 Hz, CH), 3.22 (1H, d, $^2J_{HH}$ = 6.5 Hz, CH), 3.55 (2H, t, $^3J_{HH}$ = 6.8 Hz, 2CH), 3.65 (6H, s, 2CH$_3$O), 3.75 (6H, s, 2CH$_3$O), 5.80 (2H, s, 2CH), 9.44 (1H, s, NH). ^{13}C NMR (125.7 MHz, $CDCl_3$): δ_{ppm} 166.8, 165.3, 154.0, 137.7, 130.2, 121.4, 111.2, 53.0, 51.6, 41.1, 32.1, 28.1, 11.3. MS, *m*/*z* (%): 487 (M$^+$, 10), 31 (100). Anal. calcd for $C_{24}H_{29}N_3O_8$ (487.51): C, 59.13; H, 6.00; N, 8.62; found: C, 59.24; H, 6.27; N, 8.72%.

2.3.5 Dimethyl 6-imino-2,10-bis(4-nitrophenyl)-10,12-dihydro-2*H*,6*H*-dipyrido[1,2-*c*:2′,1′-*f*]pyrimidine-3,9-dicarboxylate (5e). Yellow powder, m. p. 159–161 °C, yield: 75%. IR (KBr) (ν_{max}/cm^{-1}): 3445, 1739, 1736, 1486, 1376 and 1290. ^{1}H NMR (500 MHz, $CDCl_3$): δ_{ppm} 3.08 (1H, d, $^2J_{HH}$ = 6.5 Hz, CH), 3.17 (1H, d, $^2J_{HH}$ = 6.5 Hz, CH), 3.67 (6H, s, 2CH$_3$O), 4.80 (2H, s, 2CH), 6.03 (2H, s, 2CH), 7.54 (4H, d, $^3J_{HH}$ = 7.6 Hz, 4CH), 8.18 (4H, d, $^3J_{HH}$ = 7.6 Hz, 4CH), 8.25 (1H, s, 1CH), 8.67 (1H, s, NH). ^{13}C NMR (125.7 MHz, $CDCl_3$): δ_{ppm} 166.4, 152.9, 150.3, 146.6, 136.1, 135.4, 133.4, 129.3, 123.2, 109.7, 51.7, 39.8, 29.9. MS, *m*/*z* (%): 557 (M$^+$, 10), 31 (100). Anal. calcd for $C_{28}H_{23}N_5O_8$(557.52): C, 60.32; H, 4.16; N, 12.56; found: C, 60.45; H, 4.26; N, 12.67%.

2.3.6 Tetramethyl 6-imino-2,10-bis(4-methoxyphenyl)-10,12-dihydro-2*H*,6*H*-dipyrido[1,2-*c*:2′,1′-*f*]pyrimidine-3,4,8,9-tetracarboxylate (5f). Yellow powder, m. p. 147–149 °C, yield: 90%. IR (KBr) (ν_{max}/cm^{-1}): 3442, 1740, 1738, 1578, 1475 and 1286. ^{1}H NMR (500 MHz, $CDCl_3$): δ_{ppm} 3.14 (1H, d, $^2J_{HH}$ = 6.5 Hz, CH), 3.21 (1H, d, $^2J_{HH}$ = 6.5 Hz, CH), 3.62 (6H, s, 2CH$_3$O), 3.68 (6H, s, 2CH$_3$O), 3.78 (6H, s, 2CH$_3$O), 4.73 (2H, s, CH$_2$), 6.03 (2H, s, 2CH), 6.86 (4H, d, $^3J_{HH}$ = 7.6 Hz, 4CH), 7.11 (4H, d, $^3J_{HH}$ = 7.6 Hz, 4CH), 9.44 (1H, s, NH). ^{13}C NMR (125.7 MHz, $CDCl_3$): δ_{ppm} 165.9, 165.1, 159.0, 154.1, 140.7, 137.7, 136.2, 129.5, 121.0, 115.6, 114.4, 55.3, 53.0, 51.6, 38.6, 32.2. MS, *m*/*z* (%): 634 (M$^+$, 10), 31 (100). Anal. calcd for $C_{34}H_{33}N_3O_{10}$ (634.65): C, 63.45; H, 5.17; N, 6.53; found: C, 63.58; H, 5.26; N, 6.68%.

2.3.7 Tetramethyl 6-imino-2,10-bis(4-nitrophenyl)-10,12-dihydro-2*H*,6*H*-dipyrido[1,2-*c*:2′,1′-*f*]pyrimidine-3,4,8,9-tetracarboxylate (5g). Yellow powder, m. p. 178–179 °C, yield: 75%. IR (KBr) (ν_{max}/cm^{-1}): 3358, 1738, 1735, 1487 and 1268. ^{1}H NMR (500 MHz, $CDCl_3$): δ_{ppm} 3.15 (1H, d, $^2J_{HH}$ = 6.7 Hz, CH), 3.20 (1H, d, $^2J_{HH}$ = 6.7 Hz, CH), 3.63 (6H, s, 2CH$_3$O), 3.74 (6H, s, 2CH$_3$O), 4.79 (2H, s, 2CH), 5.98 (2H, s, 2CH), 7.52 (4H, d, $^3J_{HH}$ = 7.6 Hz, 4CH), 8.16 (4H, d, $^3J_{HH}$ = 7.6 Hz, 4CH), 9.45 (1H, s, NH). ^{13}C NMR (125.7 MHz, $CDCl_3$): δ_{ppm} 165.9, 165.1, 154.1, 149.5, 146.6, 140.7, 137.1, 129.2, 124.4, 120.9, 115.6, 53.0, 51.6, 38.6, 32.2. MS, *m*/*z* (%): 802 (M$^+$, 10), 45 (100). Anal. calcd for $C_{32}H_{27}N_5O_{12}$ (673.59): C, 57.06; H, 4.04; N, 10.40; found: C, 57.22; H, 4.18; N, 10.52%.

2.3.8 Dimethyl 6-imino-2,10-di-*p*-tolyl-10,12-dihydro-2*H*,6*H*-dipyrido[1,2-*c*:2′,1′-*f*]pyrimidine-3,9-dicarboxylate (5h). Pale yellow powder, m. p. 139–141 °C, yield: 90%. IR (KBr) (ν_{max}/cm^{-1}): 3452, 1742, 1739 and 1487. ^{1}H NMR (500 MHz, $CDCl_3$): δ_{ppm} 2.35 (6H, s, 2Me), 3.09 (1H, d, $^2J_{HH}$ = 6.7 Hz, CH), 3.17 (1H, d, $^2J_{HH}$ = 6.7 Hz, CH), 3.67 (6H, s, 2CH$_3$O), 4.80 (2H, s, CH$_2$), 6.03 (2H, s, 2CH), 7.14 (4H, d, $^3J_{HH}$ = 7.6 Hz, 4CH), 7.17 (4H, d, $^3J_{HH}$ = 7.6 Hz, 4CH), 8.25 (1H, s, 1CH), 9.44 (1H, s, NH). ^{13}C NMR (125.7 MHz, $CDCl_3$): δ_{ppm} 166.4, 151.9, 140.6, 137.8, 136.1, 134.4, 134.2, 130.1, 128.5, 122.9, 109.7, 51.6, 39.8, 21.1. MS, *m*/*z* (%): 495 (M$^+$, 10), 31 (100). Anal. calcd for $C_{30}H_{29}N_3O_4$ (495.58): C, 72.71; H, 5.90; N, 8.48; found: C, 72.83; H, 5.98; N, 8.56%.

2.3.9 Diethyl 6-imino-2,10-dimethyl-10,12-dihydro-2*H*,6*H*-dipyrido[1,2-*c*:2′,1′-*f*]pyrimidine-3,9-dicarboxylate (5i). Pale yellow powder, m. p. 133–135 °C, yield: 85%. IR (KBr) (ν_{max}/cm^{-1}): 1739, 1737, 1695, 1576, 1368 and 1284. ^{1}H NMR (500 MHz, $CDCl_3$): δ_{ppm} 1.22 (6H, t, $^3J_{HH}$ = 7.3 Hz, 2CH$_3$), 1.27 (6H, d, $^3J_{HH}$ = 6.8 Hz, 2CH$_3$), 2.97 (1H, d, $^2J_{HH}$ = 6.7 Hz, CH), 3.05 (1H, d, $^2J_{HH}$ = 6.7 Hz, CH), 3.65 (2H, q, $^3J_{HH}$ = 7.2 Hz, 2CH), 4.21 (4H, q, $^3J_{HH}$ = 7.2 Hz, 2CH$_2$O), 5.80 (2H, s, CH), 8.23 (1H, s, CH), 8.67 (1H, s, NH). ^{13}C NMR (125.7 MHz, $CDCl_3$): δ_{ppm} 167.3, 151.6, 140.8, 134.7, 126.0, 112.2, 61.8, 49.3, 26.8, 19.6, 14.1. MS, *m*/*z* (%): 890 (M$^+$, 10), 45 (100). Anal. calcd for $C_{20}H_{25}N_3O_4$ (371.44): C, 64.67; H, 6.78; N, 11.31; found: C, 64.85; H, 6.86; N, 11.45%.

2.3.10 Diethyl 6-imino-2,10-bis(4-methoxyphenyl)-10,12-dihydro-2*H*,6*H*-dipyrido[1,2-*c*:2′,1′-*f*]pyrimidine-3,9-dicarboxylate (5j). Pale yellow powder, m. p. 151–153 °C, yield: 90%. IR (KBr) (ν_{max}/cm^{-1}): 1742, 1739, 1587, 1378 and 1292. ^{1}H NMR (500 MHz, $CDCl_3$): δ_{ppm} 1.22 (6H, t, $^3J_{HH}$ = 7.3 Hz, 2CH$_3$), 3.08 (1H, d, $^2J_{HH}$ = 6.2 Hz, CH), 3.17 (1H, d, $^2J_{HH}$ = 7.3 Hz, CH), 3.78 (6H, s, 2OCH$_3$), 4.12 (4H, q, $^3J_{HH}$ = 7.3 Hz, 2CH$_2$O), 4.78 (2H, s, 2CH), 6.04 (2H, s, 2CH), 6.86 (4H, d, $^3J_{HH}$ = 7.6 Hz, 4CH), 7.18 (4H, d, $^3J_{HH}$ = 7.6 Hz, 4CH), 8.15 (1H, s, CH), 8.67 (1H, s, NH). ^{13}C NMR (125.7 MHz, $CDCl_3$): δ_{ppm} 166.6, 159.0, 151.9, 140.8, 136.1, 135.4, 129.6, 123.1, 114.4, 110.1, 61.7, 55.3, 49.8, 43.4, 14.1. MS, *m*/*z* (%): 555 (M$^+$, 10), 45 (100). Anal. calcd for $C_{32}H_{33}N_3O_6$ (890.94): C, 69.17; H, 5.99; N, 7.56; found: C, 69.32; H, 6.12; N, 7.72%.

2.4. Evaluation of antioxidant property *via* DPPH

In this investigation, the antioxidant capabilities of a series of synthesized dipyridopyrimidines (specifically compounds **5a–5d**) were assessed utilizing the DPPH free radical scavenging assay, adhering to methodologies established by Shimada *et al.*[81] Dipyridopyrimidines **5a–5d** were examined across a concentration gradient of 200 to 1000 ppm, consistent with the Shimada protocol. Subsequently, an equal volume of a methanolic DPPH solution (1 mmol L^{-1}) was introduced to the dipyridopyrimidine solution. Post-incubation at ambient temperature in darkness for a duration of 30 minutes with agitation, the absorbance of the resulting mixture was quantified spectrophotometrically at a wavelength of 517 nm. To contextualize the antioxidant activity of the synthesized dipyridopyrimidines **5a–5d**, their performance was benchmarked against established antioxidants butylated hydroxytoluene (BHT) and 2-*tert*-butylhydroquinone (TBHQ). Control measurements utilized methanol (3 mL) *in lieu* of the synthesized compounds. Finally, the percentage of DPPH radical scavenging inhibition was calculated according to the formula articulated by Yen and Duh.[82]

2.5. Evaluating FRAP process of dipyridopyrimidines antioxidant activity

Employing the DPPH free radical assay, in conjunction with methodologies established by Yildirim *et al.*,[83] the present study delves into the antioxidant properties exhibited by a series of newly synthesized dipyridopyrimidines, specifically compounds **5a–5d**. Dipyridopyrimidines **5a–5d** were evaluated at concentrations ranging from 200 to 1000 ppm, adhering to the parameters outlined in the Shimada method. Subsequently, an aliquot of the dipyridopyrimidine solution was combined with an equivalent volume of a 1 mmol per L DPPH solution prepared in methanol. The resulting mixture, after incubation in darkness for 30 minutes at ambient temperature, underwent spectrophotometric analysis at 517 nm to determine its absorbance. In order to ascertain the antioxidant efficacy of dipyridopyrimidines **5a–5d**, a comparative analysis was undertaken utilizing TBHQ and BHT as reference standards, with methanol (3 mL) serving as the blank control *in lieu* of the synthesized compounds.

2.6. Examining antibacterial activity of the prepared dipyridopyrimidines

Employing the disk diffusion method, a Persian-type culture collection (PTCC) comprising both Gram-positive and Gram-negative bacteria was established. This investigation aimed to ascertain the antibacterial activity of selected dipyridopyrimidines, namely compounds **5a**, **5d**, **5e**, and **5h**. To assess the aforementioned dipyridopyrimidines' efficacy, bacterial cultures were cultivated at 37 °C for a period of 16 to 24 hours, adhering to the McFarland Standard No. 0.5 preparation protocol. Streptomycin and gentamicin served as the principal antimicrobial agents for comparative analysis. A bacterial suspension was prepared by inoculating a disinfected swab onto Mueller Hinton agar, conforming to the McFarland Standard No. 0.5 (1.5×10^8 CFU mL^{-1}). Subsequent to the application of dipyridopyrimidines **5a**, **5d**, **5e**, and **5h** (at a concentration of 25 μg mL^{-1}) onto sterile blank disks to evaluate their antibacterial characteristics, the specimens underwent incubation at 37 °C for 24 hours. The resulting zones of inhibition were then measured and contrasted with those observed in the control group.

2.7. Catalytic performance of the Cu/ZnO@GO in organic pollutants such as 4-NP reduction

In a typical experimental run, a mixture comprising 25 mL of 4-nitrophenol solution (2.5 mM) and 5.0 mg of Cu/ZnO@GO catalyst was prepared within a beaker and left undisturbed at ambient temperature for a period of 2 minutes. Subsequently, the reaction was initiated by the introduction of 25 mL of a freshly prepared 0.25 M $NaBH_4$ solution into the same beaker. Upon addition of the $NaBH_4$ solution, an immediate visual transformation occurred, with the solution's color changing almost instantaneously from a pale yellow to a more vibrant lemon-yellow shade. This mixture underwent continuous stirring until complete decolorization was observed. Post-decolorization, a 1 mL aliquot of the solution was subjected to a 25-fold dilution to enable subsequent absorbance measurements *via* UV-Vis spectroscopy at predetermined time points. The temporal variation in 4-nitrophenol concentration was monitored by recording UV-Vis absorption spectra over a wavelength range of 200 to 700 nm, maintaining room temperature throughout the analysis. To assess the recyclability of the catalyst, it was recovered *via* filtration, thoroughly rinsed with ethanol, dried to remove residual solvent, and then subjected to repeated catalytic cycles.

3. Results and discussion

The current investigation focused on the synthesis of a series of dipyridopyrimidines **5a–5j** *via* a four-component reaction involving acetylacetone **1**, aldehydes **2**, guanidine **3**, and activated acetylenic compounds **4**, conducted in aqueous media at ambient temperature (Scheme 1). The reactions, occurring in an aqueous milieu at standard room temperature (Scheme 1), employed Cu/ZnO@GO as a recoverable nanocatalyst. High efficiency characterized the production of the targeted compounds. The catalytic efficacy of the Cu/ZnO@GO nanocatalyst was evaluated through its capacity to facilitate dipyridopyrimidine formation. The generated catalyst, Cu/ZnO@GO, contains Lewis acid sites (Cu and Zn) that help in the nucleophilic attack on active carbonyl groups, along with a Lewis base site (O) which effectively eliminates acid hydrogen from the reactants, leading to the formation of intermediates. Additionally, metal oxides show high crystallinity, which is vital for their catalytic effectiveness, and the synergy of two or more metals along with different processing techniques enhances the surface characteristics of the materials, making them suitable for targeted applications. The newly created Cu/ZnO@GO nanocatalyst was thoroughly characterized using various

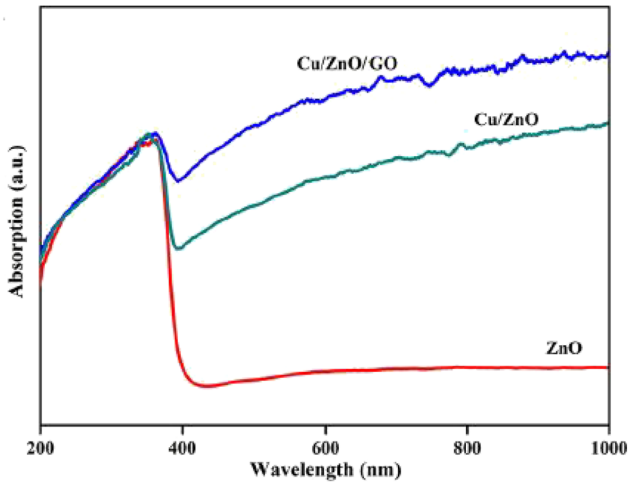

Fig. 1 FT-IR (KBr) spectra of Cu/ZnO@GO.

analytical methods. Characterization techniques employed included X-ray diffraction (XRD), energy dispersive X-ray spectrometry (EDS), Fourier-transform infrared spectroscopy (FT-IR), transmission electron microscopy (TEM), and field emission scanning electron microscopy (FE-SEM). The FT-IR spectra of ZnO, Cu@ZnO, and Cu/ZnO@GO samples are presented in (Fig. 1). Prominent peaks observed at 3330 cm^{-1} and 3337 cm^{-1} correspond to the H–O–H stretching vibrations associated with water molecules incorporated within the synthesized particles. Spectral signatures at 1020 cm^{-1} and 652.17 cm^{-1} are indicative of metal–oxide–metal vibrational modes, specifically those associated with Zn–O–Zn and Zn–O–Cu stretching. Vibrations detected at 465 cm^{-1} and 455 cm^{-1} are ascribed to the [M–O] vibrations of the metal oxides, corresponding to Zn–O.

The X-ray diffraction patterns for the Cu/ZnO@GO nanocatalyst are shown in (Fig. 2). The lack of a clear structure in the Cu/ZnO@GO particles can be linked to the gradual layering of Cu nanoparticles and ZnO on the graphene oxide (GO) surface.

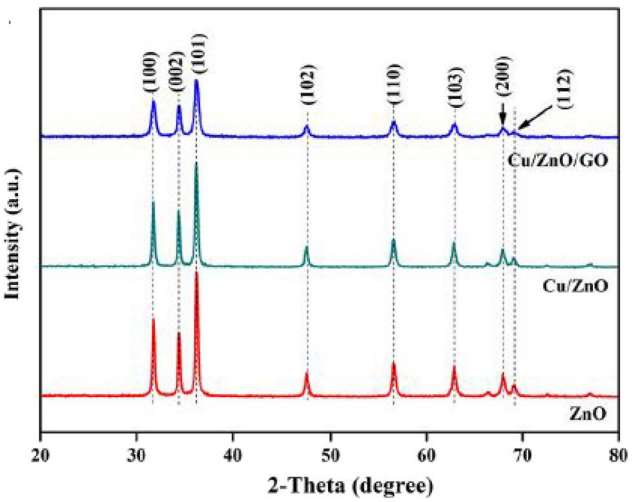

Fig. 2 X-ray diffraction patterns of Cu/ZnO@GO.

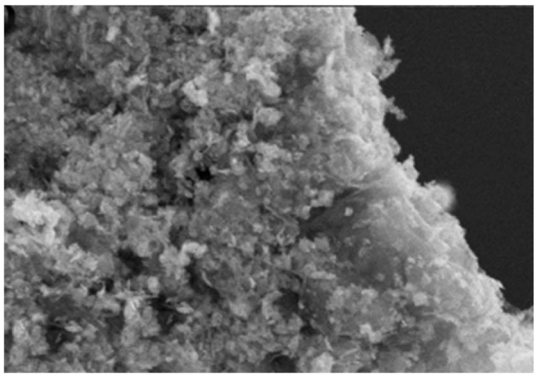

Fig. 3 The FESEM analysis of Cu/ZnO@GO.

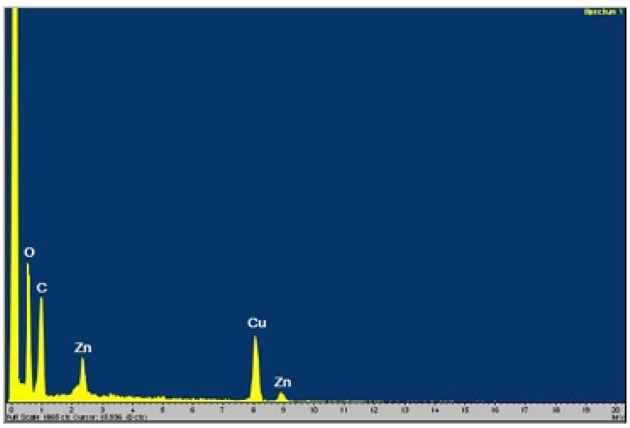

Fig. 4 The EDX analysis of Cu/ZnO@GO.

The strong peaks observed further support the small size and nanoscale characteristics of the particles. Specific peaks in the X-ray diffraction (XRD) pattern of the nanocatalyst relate to the ZnO and Cu nanoparticles. The ZnO peaks are correctly matched to the hexagonal phase with a wurtzite structure, as specified in JCPDS No. 01-082-9744. The peaks for Cu match the standard powder diffraction card noted as JCPDS No. 01-087-0717. As shown in Fig. 2, adding Cu leads to a decrease in the peak intensities for the main planes linked to ZnO (100), (002), and (101).

Cu/ZnO@GO FESEM images are shown in (Fig. 3), providing tangible evidence of the nanocatalyst effective production.

Utilizing energy-dispersive X-ray (EDX) spectroscopic analysis, the relative abundance and chemical composition of the various constituents within the nanocatalyst were determined (see Fig. 4). The results from this analysis strongly suggest that the synthesis of Cu@ZnO@GO was successfully achieved. As illustrated in Fig. 4, the presence of copper (Cu), zinc (Zn), oxygen (O), and carbon (C) elements was identified.

Furthermore, elemental mapping was performed to examine the spatial distribution of these elements within the Cu@ZnO@GO nanocatalyst (refer to Fig. 5). This analysis corroborated the previous findings, confirming with high clarity that Cu, Zn, O, and C were distributed throughout the material with

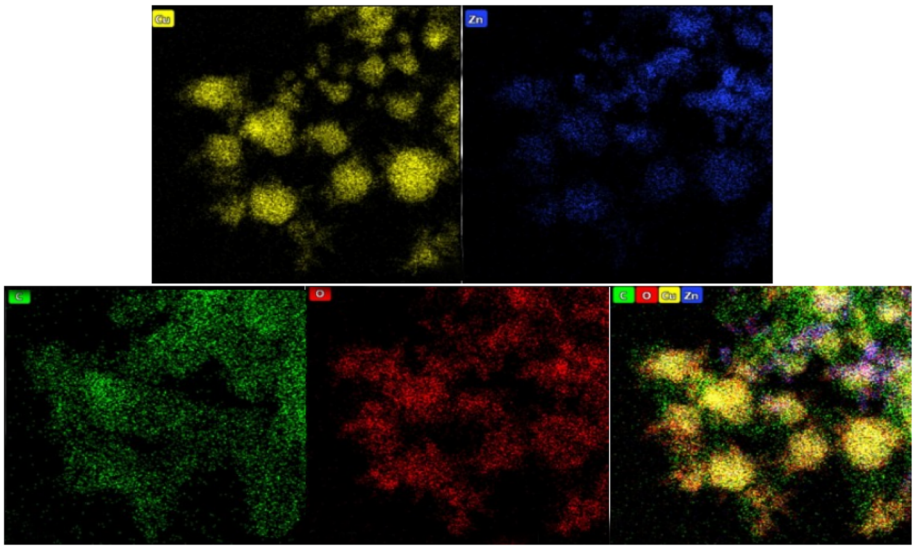

Fig. 5 EDS mapping analysis of Cu/ZnO@GO.

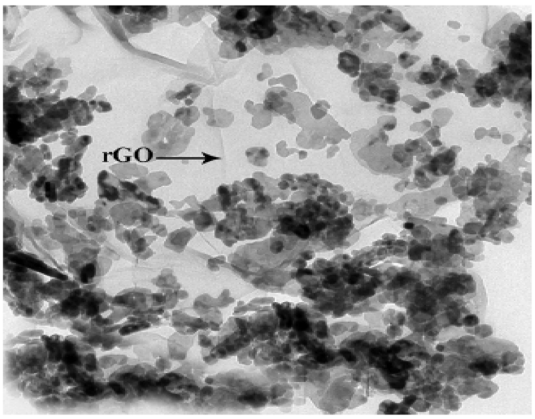

Fig. 6 TEM images analysis of Cu/ZnO@GO.

a suitable degree of dispersity. Consequently, the outcomes derived from the elemental mapping convincingly validated the initial EDX analysis, thereby reinforcing the reliability of the elemental composition data.

To conduct a more detailed analysis of the morphological characteristics of the Cu@ZnO/GO nanocatalyst, Transmission Electron Microscopy (TEM) was employed to examine the samples, as illustrated in (Fig. 6). The results indicate that the Cu@ZnO nanoparticles are effectively anchored onto the GO support.

In the field of organic chemistry, optimizing reaction conditions is essential because it significantly influences the effectiveness and outcome of the experiments. To achieve this, we initially chose the experimental model including acetylacetone **1**, acetaldehyde **2a**, guanidine **3**, and dimethyl acetylenedicarboxylate **4a** (refer to Table 1). Even after a period of 10 hours, the amount of compound **5a** without any catalyst is trace (entry 1, Table 1). To support this observation, we introduced a catalyst with 0.01 g of Cu nanoparticles into the reaction mixture. The successful synthesis of dipyridopyrimidine **5a**, as detailed in entry 3 of Table 1, was achieved with notable efficacy (45%) within a 3-hour reaction period. Consequently, the presence of a catalyst proved indispensable for facilitating

Table 1 Determining the best conditions, including catalyst, amount of catalyst and temperature for the synthesis of **5a**

Entry	Catalyst	Temp. (°C)	Catalyst (g)	TON	TOF	Time (h)	[a]Yield%
1	None	r. t.	—	—	—	10	Trace
2	None	100	—	—	—	10	Trace
3	Cu NPs	r. t.	0.01	45	15	3	45
4	ZnO NPs	r. t.	0.015	37.3	12.4	3	56
5	ZnO NPs	r. t.	0.02	32.5	10.8	3	65
6	ZnO NPs	r. t.	0.025	26	8.67	3	65
7	ZnO@MWCNTs	r. t.	0.02	35	11.67	3	70
8	MWCNTs	r. t.	0.02	12.5	4.17	3	25
9	Cu@ MWCNTs	r. t.	0.02	27.5	9.17	3	55
10	Cu/ZnO	r. t.	0.02	39	13	3	78
11	Cu/ZnO@GO	r. t.	0.02	42.5	14.17	3	85
12	Cu/ZnO@GO	100	0.02	42.5	14.18	3	85

[a] Isolated yields.

Table 2 Determining the best solvent for generation of **5a**

Entry	Solvent	Time (h)	[a]Yield%
1	EtOH	15	78
2	CH_2Cl_2	8	75
3	$CHCl_3$	5	75
4	**H_2O**	**3**	**85**
5	Solvent-free	8	60
6	DMF	12	45
7	Toluene	12	75
8	CH_3CN	5	87

[a] Isolated yields.

Table 3 Reusability of catalyst for synthesis of compound **5a**

Run	% yield[a]
1st	85
2nd	85
3rd	85
4th	80
5th	78

[a] Isolated yields.

favorable reaction outcomes. An extensive evaluation was undertaken involving a range of nanocatalysts, including copper nanoparticles (NPs), zinc oxide (ZnO), and related materials. Specifically, ZnO@MWCNTs and ZnO/Cu nanoparticles (NPs) were explored to ascertain the optimal catalyst for the model reaction. Cu/ZnO@GO nanocatalyst was ultimately selected for the synthesis of dipyridopyrimidine **5a**, affording an improvement in product yield. Modulation of the Cu/ZnO@GO quantity within the range of 0.01–0.03 g led to observable variations in reaction efficiency. A quantity of 0.02 g of Cu/ZnO@GO was employed in the synthesis of dipyridopyrimidine **5a**, yielding a considerable product amount, as documented in entry 11 of Table 1. As referenced in entry 11 of Table 1, compound **5a** was generated with an 85% yield following a 3-hour reaction. The application of nanocatalysts in the production of dipyridopyrimidine derivatives necessitates both Lewis acid and Lewis base functionality. The metals copper (Cu) and zinc (Zn) are capable of acting as Lewis acids, thereby activating the carbonyl group and rendering it more susceptible to nucleophilic attack.

The sample response was optimized by raising the temperature to 100 °C. However, the efficacy of dipyridopyrimidines **5a** remained unchanged as a consequence of this adjustment (entry 2 and entry 12, Table 1). Furthermore, this investigation aimed to examine the impact of solvents on the synthesis of compound **5a** when Cu/ZnO@GO (0.02 g) was present. Water is by far the best solvent for promoting the reaction, according to the data in Table 2.

Tables 1 and 2 show how effective Cu/ZnO@GO (0.02 g) is as an organometallic catalyst for creating dipyridopyrimidines **5**. The catalyst works best when utilized in an aqueous environment and at normal room temperature. A key part of generating organic compounds involves the recycling of a catalyst. Water is vital for life on Earth and serves as the preferred solvent in nature's processes. In "on-water" reactions, water does not act as a solvent but instead supports reactants on its surface in an emulsion. On-water reactions refer to a category of organic chemical reactions occurring as emulsions in water. This concept has been recognized since 2005 when researchers from K. Barry Sharpless's team conducted a detailed study on this topic.[84] Unlike in-water reactions, lipophilic substances cluster together to create a watery suspension (on water). When surfactants form a self-organized aggregate to hold lipophilic reactants, it is possible to differentiate reactions that take place inside this aggregate. In these cases, hydrogen bonding can play a role in enhancing reactions in water. By increasing the number of hydrogen bonds through a larger interfacial area, the speed of the reaction should also improve. Indeed, the same researchers showed through optical measurements that the stirring rate is linked to the interfacial area in the reaction between cyclopentadiene and methyl acrylate in water. They found that as these values increased, so did the conversion rates.[85,86] Table 3 demonstrates the successful use of the prepared nanocatalyst in the research to produce dipyridopyrimidines **5a** across four different trials. The nanocatalyst was removed from the reaction mixture through filtration and was set up for reuse. It should then be rinsed with water and left to dry in the air for an entire day at room temperature. After that, it can be applied for future uses.

Through close observation, the process of measuring catalyst leaching can be done by using hot filtration. It is best to take out the catalyst from the mixture once the reaction's conversion rate hits 54%. Catalyst leaching occurs if the reaction keeps going. On the other hand, if the reaction stops, it can be said that leaching is not a concern (Fig. 7).

To ascertain the precise chemical composition of the synthesized dipyridopyrimidine compound **5**, a comprehensive suite of analytical methodologies was implemented. These included proton nuclear magnetic resonance (^{1}HNMR)

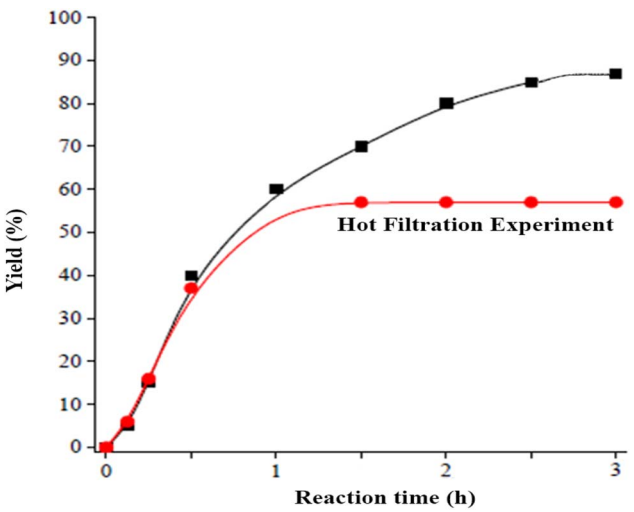

Fig. 7 Hot filtration of Cu/ZnO@GO.

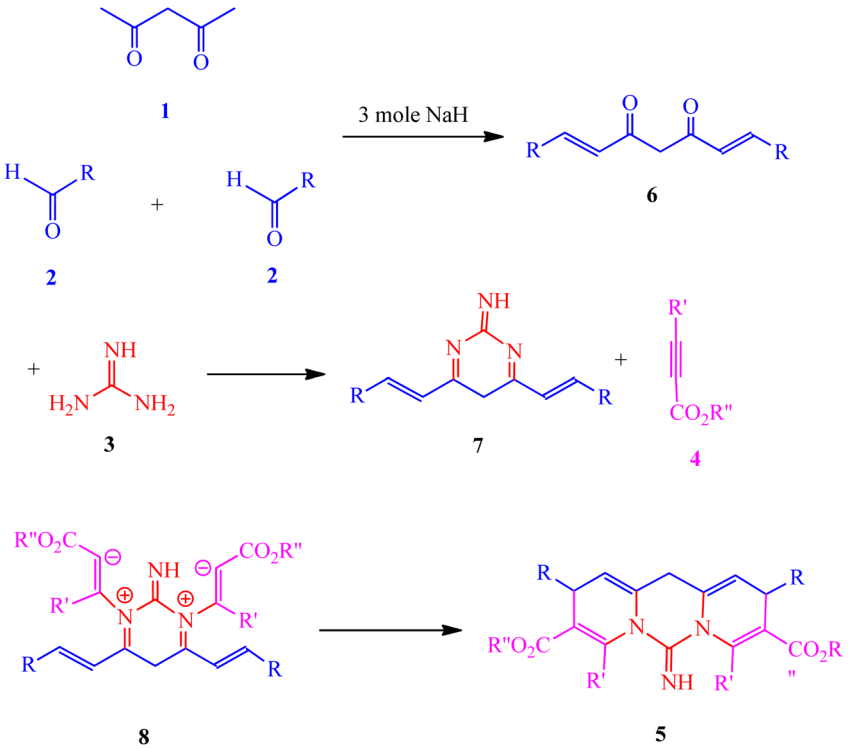

Scheme 2 Proposed mechanism for the formation of **5**.

spectroscopy, carbon-13 nuclear magnetic resonance (^{13}CNMR) spectroscopy, infrared (IR) spectroscopy, elemental analysis, and mass spectrometry. Analysis of the ^{1}HNMR spectra of dipyridopyrimidines revealed that compound **5a** exhibited a doublet signal at 1.25 ppm, a characteristic feature indicative of protons within two methyl (CH_3) groups. A two-doublet peak was also observed at 3.07 and 3.18 ppm, corresponding to two methylene protons diastereotopic. Furthermore, two singlet peaks at 3.65 and 3.75 ppm were recorded, attributable to methoxy groups, alongside another singlet at 9.44 ppm, indicative of NH protons. Examination of the ^{13}CNMR spectra of compound **5a** led to the identification of a single resonance for the C=NH group, with chemical shifts registered at 153.9 ppm and C=O groups at 166.7 and 165.5 ppm. Moreover, infrared (IR) spectroscopy provided valuable corroboration regarding the presence of specific functional groups inherent to the molecular structure of the compound. Scheme 2 provides a clear illustration of the most efficacious procedure employed for the generation of the synthesized compounds **5**. The current experimental investigation involves the reaction of unsaturated

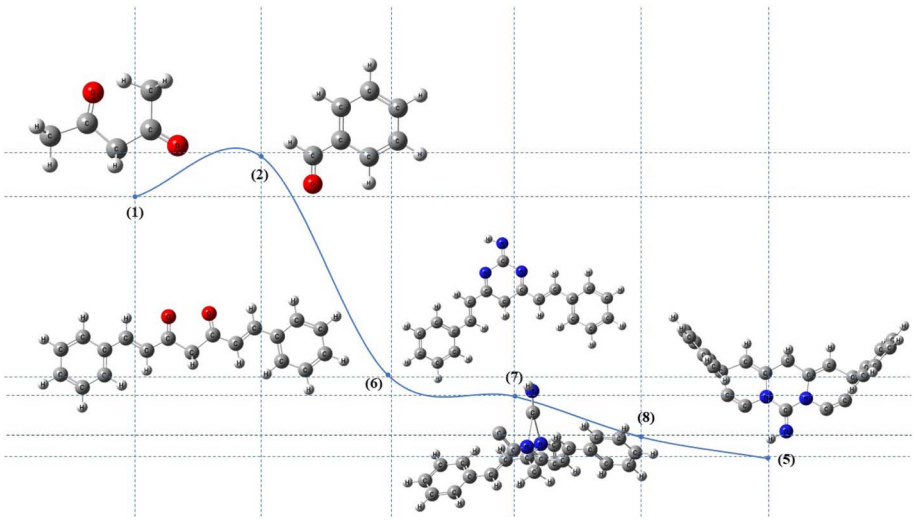

Scheme 3 Profile of the activated intermediates for the formation of **5** that calculated by B3LYP/6-311G(d,P) level of theory.

acetylacetone **1**, aldehydes **2**, and Cu/ZnO@GO (0.02 g), yielding intermediate **6**, which subsequently reacts with guanidine **3** to produce intermediate **7**. Intermediate **7** and activated acetylenic compounds **4** react and produced intermediate **8.** This intermediate **8** then undergoes an intermolecular cyclization reaction, ultimately resulting in the formation of compound **5**.

The theoretical investigation of proposed reaction mechanism depicted in Scheme 3, illustrates the reaction pathway by charting the total energy landscape between reactants and products. The pathway suggests a mechanism proceeding *via* the formation of six distinct intermediates. These activated intermediates were subjected to optimization at the B3LYP/6-311G(d,p) level of theory, corroborating the proposed mechanism through an assessment of the intermediates' stability and the feasibility of their formation.[87–89]

3.1. Catalytic performance of the Cu/ZnO@GO in 4-NP reduction

To scrutinize the catalytic behavior of synthesized Cu/ZnO@GO within an aqueous medium at ambient temperature, 4-nitrophenol was selected as a model substrate in this investigation. The progression of the reduction processes involving the dye was monitored *via* alterations in the UV-vis absorption spectrum of the reaction mixture, maintained at room temperature, following the removal of the catalyst through centrifugation. Initially, the transformation of 4-nitrophenol into 4-aminophenol (4-AP) was examined, utilizing Cu/ZnO@GO as the catalyst in a model reaction. Control experiments, wherein the catalyst was excluded but $NaBH_4$ was present, yielded negligible conversion, thus underscoring the indispensable role of Cu/ZnO@GO in facilitating the reduction of 4-nitrophenol to 4-aminophenol. The reaction's advancement was quantified using UV-vis spectroscopy, and the resultant data is presented graphically in (Fig. 8). Characteristically, 4-nitrophenol exhibited an absorption maximum at 317 nm in aqueous solution. Upon the introduction of freshly prepared aqueous $NaBH_4$ solution, a bathochromic shift in the 4-nitrophenol absorption band from 317 nm to 400 nm was observed, concomitant with a noticeable color transition from light yellow to bright yellow, indicative of 4-nitrophenolate ion formation. Notably, in the absence of Cu/ZnO@GO, the absorption peak at 400 nm remained unaltered even after a 15-hour period. This observation suggests that $NaBH_4$, despite its potency as a reducing agent, is incapable of reducing the 4-nitrophenolate ion in the absence of the catalyst, even with the presence of an electron donor (BH_4^-) and a proton source (H_2O) within the reaction milieu. Furthermore, the absorbance of a 4-nitrophenol solution remained constant over several hours when Cu/ZnO@GO was introduced in the absence of $NaBH_4$. However, when both Cu/ZnO@GO and $NaBH_4$ were present, the absorbance at 400 nm quickly dropped to nearly zero within 10 minutes, while a new peak appeared around 300 nm, attributed to 4-aminophenol, and increased gradually as the yellow color of the solution faded.

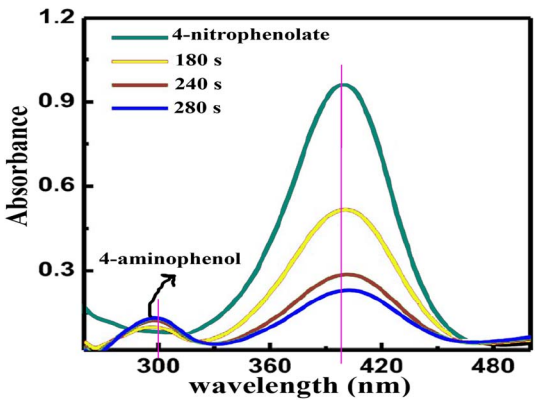

Fig. 8 UV-vis spectrum of reduction of 4-nitrophenol and photocatalytic reduction of the 4-NP.

In light of these considerations, Cu/ZnO@GO was employed in this study to facilitate the photocatalytic reduction of 4-nitrophenol (4-NP). The prepared Cu/ZnO@GO composite microspheres demonstrated superior photocatalytic activity compared to their counterparts, an enhancement attributed to the synergistic advantages conferred by the incorporation of copper nanoparticles (Cu NPs), which augment light absorption. Significantly, these composite microspheres are amenable to facile removal from the reaction medium *via* external means, and subsequent reuse demonstrated only marginal diminution in catalytic efficacy. Consequently, these findings suggest that Cu/ZnO@GO composite microspheres present a viable, environmentally benign, and economically attractive approach for the elimination and photoreduction of 4-NP.

3.2. Assessing the antioxidant capacity of synthesized dipyridopyrimidines using the DPPH method

Additionally, the goal of this study was to explore the antioxidant properties of the synthesized dipyridopyrimidines. To achieve this goal, the DPPH test was used. The DPPH radical scavenging method is a common technique for measuring the antioxidant strength of synthetic substances, food products, and biological materials.[90,91] This experiment investigates how the DPPH free radical interacts with the sample being tested. In this process, the sample has the ability to take in either an electron or a hydrogen atom from the DPPH radical. The dipyridopyrimidines showed their antioxidant abilities because they could lose an electron or a hydrogen atom in the presence of the DPPH radical. The relative antioxidant activity is assessed by how well the created dipyridopyrimidines can capture DPPH free radicals. This research involved evaluating the antioxidant properties of a set of synthetic compounds, specifically **5a–5d**. We compared the antioxidant activity of these compounds with the known antioxidants BHT and TBHQ. The measurement of antioxidant activity was conducted by assessing how these compounds absorbed electrons or hydrogen using the DPPH radical method. When an electron or hydrogen atom is added to the DPPH, its absorbance at a wavelength of 517 nm decreases. The antioxidant effectiveness of dipyridopyrimidine derivatives **5a–5d** was arranged in this way: TBHQ and BHT showed

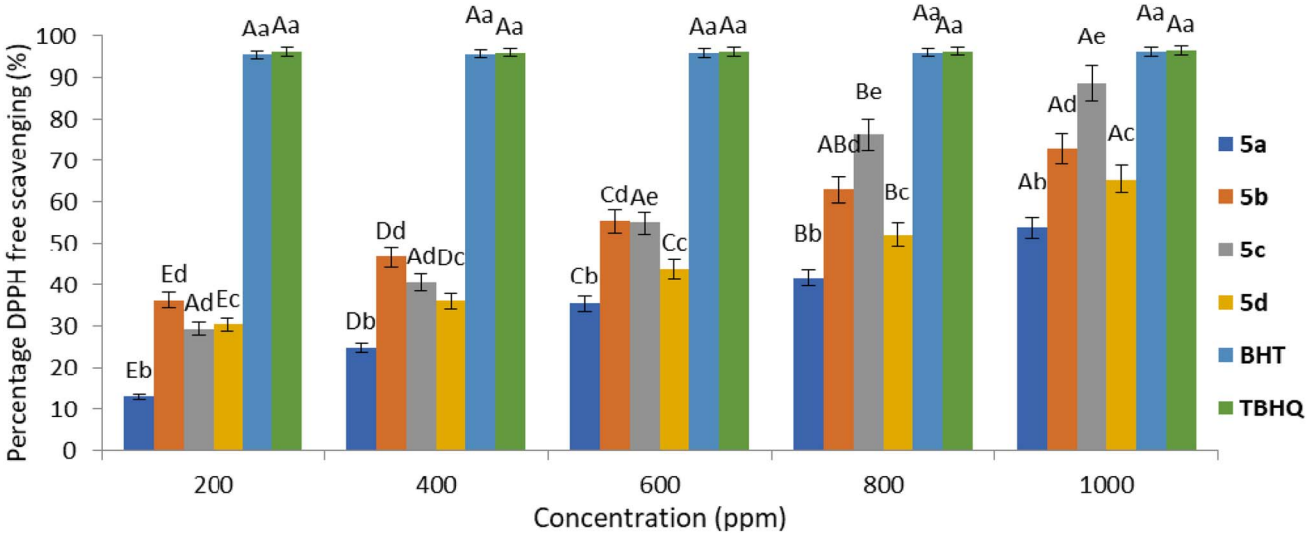

Fig. 9 Order of antioxidant activity of **5a–5d** using DPPH.

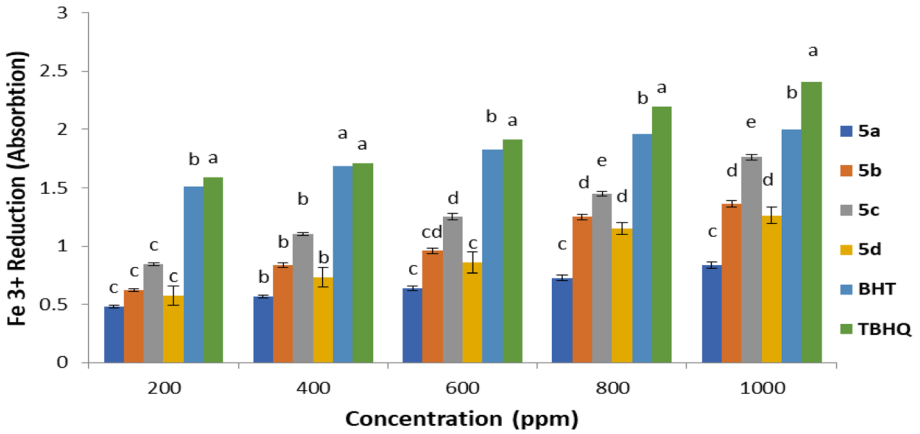

Fig. 10 Ferric ions (Fe^{3+}) decreasing antioxidant ability (FRAP) of compounds **5a–5d**.

comparable antioxidant strengths, while **5a–5d** had slightly lower capabilities, as shown in Fig. 9.

The data presented in Fig. 8 indicate notable disparities in the levels of dipyridopyrimidines in comparison to BHT and TBHQ, which are widely employed as conventional antioxidants. Within the tested group of dipyridopyrimidines, compounds **5a–5d**, compound **5c** displayed substantial efficacy in contrast to BHT and TBHQ.

3.3. Assessment of dipyridopyrimidines antioxidant activity using Fe^{3+} reducing

To ascertain the antioxidant efficacy of dipyridopyrimidines **5a–5d**, an alternative methodological approach was implemented. It was observed that these compounds facilitated the reduction of ferric ions (Fe^{3+}). The degree of this reduction was quantified by spectrophotometrically measuring the conversion of Fe^{3+}/ferricyanide to Fe^{2+}/ferrous at 700 nm. Notably, dipyridopyrimidine **5c** exhibited a significantly more pronounced positive effect than both butylated hydroxytoluene (BHT) and tertiary butylhydroquinone (TBHQ). The relative antioxidant potencies of dipyridopyrimidines **5a–5d** are presented in (Fig. 10), arrayed in the following descending order: TBHQ > BHT > **5c** > **5b** > **5d** > **5a**. It is worth noting that tertiary butylhydroquinone (TBHQ) is a structural analog of butylated hydroxytoluene (BHT).

3.4. Evaluation of antibacterial activity of synthesized dipyridopyrimidines

This investigation probed the antimicrobial efficacy of synthesized dipyridopyrimidines against both Gram-positive and Gram-negative bacterial strains. The performance of these newly synthesized compounds was benchmarked against that of streptomycin and gentamicin, commonly employed as conventional antibacterial agents. A detailed overview of the research outcomes

Table 4 Antibacterial activity of synthesized compounds 5

Compounds	*Staphylococcus aureus* (+) PTCC 1337		*Bacillus cereus* (+) PTCC 1023		*Escherichia coli* (−) PTCC1270		*Klebsiella pneumoniae* (−) PTCC 1290	
	IZ[a] (mm)	MIC[b] (μg mL^{-1})	IZ (mm)	MIC (μg mL^{-1})	IZ (mm)	MIC (μg mL^{-1})	IZ (mm)	MIC (μg mL^{-1})
5a	18 ± 0.001	25	21 ± 0.001	25	22 ± 0.002	25	16 ± 0.001	25
5b	10 ± 0.002	30	8 ± 0.002	30	10 ± 0.003	30	7 ± 0.001	30
5c	17 ± 0.086	25	19 ± 0.075	25	22 ± 0.063	25	17 ± 0.054	25
5d	20 ± 0.001	20	21 ± 0.001	20	23 ± 0.024	20	18 ± 0.002	20
5e	19 ± 0.00	20	22 ± 0.003	19	21 ± 0.001	22	19 ± 0.003	22
5f	10 ± 0.001	30	9 ± 0.001	30	9 ± 0.00	30	8 ± 0.012	30
5g	10 ± 0.023	20	9 ± 0.001	20	9 ± 0.003	20	8 ± 0.003	20
5h	18 ± 0.003	25	22 ± 0.001	25	21 ± 0.001	25	18 ± 0.001	25
5i	18 ± 0.00	25	20 ± 0.003	25	21 ± 0.00	25	19 ± 0.002	25
5j	12 ± 0.001	22	10 ± 0.00	20	10 ± 0.014	20	9 ± 0.003	22
Streptomycin	19 ± 0.00	12.5	22 ± 0.00	12.5	23 ± 0.00	12.5	21 ± 0.00	12.5
Gentamicin	20 ± 0.001	12.5	24 ± 0.00	12.5	22 ± 0.00	12.5	20 ± 0.001	12.5

[a] Zone of inhibition in diameter in mm. [b] Minimum inhibitory concentration MIC (μg mL^{-1}).

is presented in Table 4. Our analysis revealed that both the specific bacterial species under consideration and the concentration of the produced chemical entities exert a considerable influence on the resulting inhibitory zone diameter. As evidenced by the data compiled in Table 4, dipyridopyrimidines designated **5a**, **5d**, **5e**, and **5h** manifested notable antimicrobial properties effective against both Gram-positive and Gram-negative bacteria. Notably, the strongest inhibition was noted against *E. coli*, a phenomenon attributable to the substantial width of the zone of inhibition exhibited.

4. Conclusion

In overview, the synthesis of the Cu/ZnO@GO nanocatalyst was successfully achieved through a method characterized by efficiency, simplicity, cost-effectiveness, and rapidity. The formation and integrity of the nanocatalyst were extensively validated using a suite of analytical techniques, including energy-dispersive X-ray spectroscopy (EDS), X-ray diffraction (XRD), scanning electron microscopy (SEM), Fourier-transform infrared spectroscopy (FT-IR), and transmission electron microscopy (TEM). Furthermore, the potential of Cu/ZnO@GO as an innovative nanocatalyst was explored in the context of synthesizing derivatives of dipyridopyrimidines. This synthetic process yielded the desired products within a timeframe of three hours, attaining yields ranging from 70% to 90%. The advantages of this protocol encompass notably brief reaction durations, high product yields, the utilization of aqueous medium as a solvent, and alignment with principles of green chemistry. In addition, two different approaches were employed to evaluate the antioxidant activity of the synthesized dipyridopyrimidines, labeled as compounds **5a–5d**. The antimicrobial properties of these compounds were also assessed *via* disk diffusion assays against a spectrum of both Gram-positive and Gram-negative bacterial strains. To deepen the mechanistic understanding, density functional theory (DFT) calculations were performed, providing insights into the reaction pathway, the energetic landscape of key intermediates, and the overall plausibility of their formation.

Author contributions

E. Ezzatzadeh conceived the original idea and was responsible for designing the research framework. N. Karami Hezarcheshmeh carried out the research. E. Ezzatzadeh analyzed the data. R. Akbari wrote the original draft. E. Ezzatzadeh reviewed the manuscript and made edits.

Conflicts of interest

The authors declare no conflict of interest, financial or otherwise.

Data availability

The data supporting this study's findings are available in this article's SI. See DOI: **https://doi.org/10.1039/d5ra04054j**.

Acknowledgements

This research received no specific grant from funding agencies in the public, commercial, or not-for-profit sectors. The authors express their sincere gratitude for the help provided by Islamic Azad University Ardabil.

References

1 S. Zhi, X. Ma and W. Zhang, *Org. Biomol. Chem.*, 2019, **17**, 7632–7650.
2 I. A. Ibarra, A. Islas-Jácome and E. González-Zamora, *Org. Biomol. Chem.*, 2018, **16**, 1402–1418.
3 A. Maleki, *Ultrason. Sonochem.*, 2018, **40**, 460–464.
4 A. Maleki, *Helv. Chim. Acta*, 2014, **97**, 587–593.
5 A. Shaabani and A. Maleki, *Chem. Pharm. Bull.*, 2008, **56**, 79–81.

6 L. F. Tietze, C. Bsasche and K. M. Gericke, *Domino Reactions in Organic Synthesis*. Wiley-VCH, Weinheim, 2006.
7 L. Weber, M. Illgen and M. Almstetter, *Synlett*, 1999, **3**, 366–374.
8 R. P. Herrera and E. Marqués-López, *Multicomponent Reactions: Concepts and Applications for Design and Synthesis*, Wiley, Hoboken, 2015.
9 H. Fares, J. J. DiNicolantonio, J. H. O'Keefe and C. J. Lavie, *Open Heart*, 2016, **3**(2), e000473.
10 Part–IV, Studies on chalcone, **http://shodhganga.inflibnet.ac.in/bitstream/10603/2162/11/11_part4.pdf**, website accessed on 10th Mar 2014.
11 T. Bano, N. Kumar and R. Dudhe, *Org. Med. Chem.*, 2012, **2**(34), 1–6.
12 Y. Kotaiah, N. H. Krishna, K. N. Raju, C. V. Rao, S. B. Jonnalagadda and S. Maddila, *J. Korean Chem. Soc.*, 2012, **56**(1), 68–73.
13 K. Elumalai, M. A. Ali, M. Elumalai, K. Eluri and S. Srinivasan, *J. Acute Disease*, 2013, **2**, 316–321.
14 A. R. Trivedi, D. K. Dodiya, N. R. Ravat and V. H. Shah, *Arkivoc*, 2008, **11**, 131–141.
15 A. D. Khoje, A. Kulendrn, C. Charnock, B. Wan, S. Franzblau and L. L. Gundersen, *Bioorg. Med. Chem.*, 2010, **18**, 7274–7282.
16 P. K. Chaudhari, A. Pandey and V. H. Shah, *Orient. J. Chem.*, 2010, **26**(4), 1377–1383.
17 E. R. Shmalenyuk, S. N. Kochetkov and L. A. Alexandrova, *Russ. Chem. Rev.*, 2013, **82**(9), 896–915.
18 T. N. Doan and D. T. Tran, *Pharmacol. Pharm.*, 2011, **2**, 282–288.
19 M. V. JyothI, Y. R. Prasad, P. Venkatesh and M. Sureshreddy, *Chem. Sci. Trans.*, 2012, **1**(3), 716–722.
20 N. S. Rao, C. Kistareddy, B. Balram and B. Ram, *Pharma Chem.*, 2012, **4**(6), 2408–2415.
21 C. M. Bhalgat, M. Irfan Ali, B. Ramesh and G. Ramu, *Arabian J. Chem.*, 2014, **7**, 986–993.
22 J. L. Reymond and M. Awale, *ACS Chem. Neurosci.*, 2012, **3**(9), 649–657.
23 M. J. James, P. O'Brien, R. J. K. Taylor and W. P. Unsworth, *Chem.–Eur. J.*, 2016, **22**(26), 2856–2881.
24 M. E. Welsch, S. A. Snyder and B. R. Stockwell, *Curr. Opin. Chem. Biol.*, 2010, **14**, 347–361.
25 P. N. Kalaria, S. C. Karad and D. K. Raval, *Eur. J. Med. Chem.*, 2018, **158**, 917–936.
26 S. E.-S. Abbas, R. F. George, E. M Samir, M. M. A. Aref and H. A. Abdel-Aziz, *Future Med. Chem.*, 2019, **11**(18), 2395–2414.
27 A. Abdel-Aziem, M. S. El-Gendy and A. O. Abdelhamid, *Eur. J. Chem.*, 2012, **3**(4), 455–460.
28 M. Mamaghani, K. Tabatabaeian, R. Araghi, A. Fallah and R. Hossein Nia, *Org. Chem. Insights*, 2014, **2014**, 1–9.
29 A. K. Verma, A. K. Singh and M. M. Islam, *Int. J. Pharm. Sci.*, 2014, **6**(6), 341–345.
30 M. El-Shahat, E. A. Elhefny, A. A. El-Sayed and M. A. M. Salama, *Int. J. Pharm.*, 2015, **5**(1), 53–58.
31 M. B. Swami, G. R. Nagargoje, S. R. Mathapati, A. S. Bondge, A. H. Jadhav, S. P. Panchgalle and V. S. More, *J. Appl. Organomet. Chem.*, 2023, **3**(3), 184–198.
32 M. Baghayeri, A. h. Amiri, F. Karimabadi, S. Di Masi, B. Maleki, F. Adibian, A. R. Pourali and C. Malitesta, *J. Electroanal. Chem.*, 2021, **888**, 115059.
33 F. Adibian, A. R. Pourali, B. Maleki, M. Baghayeri and A. h. Amiri, *Polyhedron*, 2020, **175**, 114179.
34 B. Azizi, M. R. Poor Heravi, Z. S. Hossaini, A. G. Ebadid and E. Vessally, *RSC Adv.*, 2021, **11**, 13138–13151.
35 R. Katal, S. Masudy-Panah, M. Sabaghan, Z. S. Hossaini and M. H. Davood Abadi Farahani, *Sep. Purif. Technol.*, 2020, **250**, 117239.
36 M. Ghashghaee, M. Ghambarian and Z. Azizi, *Black Phosphorus: Synthesis, Properties and Applications*, 2020, pp. 59–72.
37 F. Zarei, S. Soleimani-Amiri and Z. Azizi, *Polycycl. Aromat. Comp.*, 2022, **42**, 6072–6089.
38 P. Ghamari Kargar, B. Maleki and M. Ghani, *ACS Appl. Nano Mater.*, 2024, **7**(8), 8765–8782.
39 R. Tayebee, E. Esmaeili, B. Maleki, A. Khoshniat, M. Chahkandi and N. Mollania, *J. Mol. Liq.*, 2020, **317**, 113928.
40 B. Maleki, R. Nejat, H. Alinezhad, S. M. Mousavi, B. Mahdavi and M. Delavari, *Org. Prep. Proced. Int.*, 2020, **52**(4), 328–339.
41 S. Mehrizi Marvast and E. Rostami, *Asian J. Green Chem.*, 2024, **8**(3), 261–277.
42 A. Zare and F. Mostaghar, *Chem. Methodol.*, 2024, **8**(1), 23–36.
43 S. Soleimani-Amiri, Z. S. Hossaini, M. Arabkhazaeli, H. Karami, S. Afshari and S. Abad, *J. Chin. Chem. Soc.*, 2019, **66**, 438–445.
44 A. B. Djurišić, X. Chen, Y. H. Leung and A. Man, *J. Mater. Chem.*, 2012, **22**, 6526–6535.
45 (*a*) B. Halliwell, *Free Radical Res.*, 1999, **31**, 261–272; (*b*) F. Ahmadi, M. Kadivar and M. Shahedi, *Food Chem.*, 2007, **105**, 57–64.
46 M. A. Babizhayev, A. I. Deyev, V. N. Yermakovea, I. V. Brikman, J. Bours and J. Bours, *Drugs R&D*, 2004, **5**, 125–139.
47 L. Liu and M. Meydani, *Nutr. Rev.*, 2002, **60**, 368–371.
48 M. Keshvari Kenari, S. Asghari, B. Maleki and M. Mohseni, *Res. Chem. Intermed.*, 2024, **50**(2), 905–924.
49 M. Ramezanpour-Touchahi, M. Mazloumi, H. Taherpour Nahzomi, F. Shirini and H. Tajik, *Chem. Methodol.*, 2024, **8**, 401–438.
50 A. Zare and R. Khanivar, *Asian J. Green Chem.*, 2024, **8**(5), 539–548.
51 S. Sajjadifar, F. Abakhsh and Z. Arzehgar, *Chem. Methodol.*, 2024, **8**(8), 550–568.
52 (*a*) A. Fathi Hasanbarogh, N. Ghasemi and E. Ezzatzadeh, *Int. J. Environ. Anal. Chem.*, 2024, **104**(17), 4911–4927; (*b*) L. Hasani, E. Ezzatzadeh and Z. S. Hossaini, *Mol. Diversity*, 2024, **28**, 4137–4149; (*c*) Z. Azizi, S. Haghpanah-Kouchesfahani, S. Nawabi, N. Daneshvar, F. Shirini and H. Tajik, *Chem. Methodol.*, 2024, **8**(9), 626–644.

53 (*a*) Z. Azizi, M. Ghashghaee and M. Ghambarian, *Black Phosphorus: Synthesis, Properties and Applications*, 2020, pp. 157–169; (*b*) H. Golipour, E. Ezzatzadeh and A. Sadeghianmaryan, *Int. J. Polym. Mater.*, 2024, **73**(11), 974–986; (*c*) S. Soleimani-Amiri, Z. S. Hossaini and Z. Azizi, *Polycyclic Aromat. Compd.*, 2023, **43**, 2938–2959.

54 (*a*) S. Ghasemi, F. Badri and H. Rahbar Kafshboran, *Asian J. Green Chem.*, 2024, **8**(1), 39–56; (*b*) R. Khazaei, A. Khazaei and M. Nasrollahzadeh, *J. Appl. Organomet. Chem.*, 2023, **3**(1), 123–133; (*c*) F. Hakimi, M. Taghvaee and E. Golrasan, *Adv. J. Chem., Sect. A*, 2023, **6**(2), 188–197; (*d*) S. Naderi, R. Sandaroos, S. Peiman and B. Maleki, *Chem. Methodol.*, 2023, **7**(5), 392–404.

55 (*a*) H. Ghafuri, M. Zargari and A. Emami, *Asian J. Green Chem.*, 2023, **7**(1), 54–69; (*b*) E. Ezzatzadeh, Z. S. Hossaini, A. Varasteh Moradi, M. Salimifard and S. Afshari-Sharif Abad, *Can. J. Chem.*, 2019, **97**(4), 270–276; (*c*) H. Shkyair Lihumis, A. Sami Abd, D. Sadiq Mahdi Al-khateeb, H. A. Mubarak, M. M. Karhib, M. Mousa Kareem and S. Abdullah Aowd, *J. Med. Pharm. Chem. Res.*, 2023, **5**, 466–482.

56 (*a*) I. Amini, V. Azizkhani, E. Ezzatzadeh, K. Pal, S. Rezayati, M. H. Fekri and P. Shirkhani, *Asian J. Green Chem.*, 2020, **4**(1), 51–59; (*b*) T. Havasi, E. Ezzatzadeh and A. Taheri, *J. Food Compos. Anal.*, 2024, **128**, 106014; (*c*) M. Farajpour, S. M. Vahdat, S. M. Baghbanian and M. Hatami, *Chem. Methodol.*, 2023, **7**(7), 540–571.

57 (*a*) A. Moshtaghi Zonouz, M. Abkar Aras, N. Jafari, Z. Rezaei and H. Hamishehkar, *RSC Adv.*, 2025, **15**, 7949; (*b*) Z. Afshari, A. Ramazani and H. Teymourinia, *Inorg. Chem. Commun.*, 2025, **172**, 113709; (*c*) I. Yavari, Z. S. Hossaini and E. Karimi, *Monatsh. Chem.*, 2007, **138**, 1267–1271.

58 (*a*) P. Ebrahimzadeh, B. Maleki, M. Ghani and S. Peiman, *Chem. Methodol.*, 2024, **8**(11), 833–855; (*b*) H. Sanaeishoar, R. Nazarpour and F. Mohave, *RSC Adv.*, 2015, **5**, 68571–68578; (*c*) M. Kamari, E. Ezzatzadeh and A. Taheri, *J. Ind. Eng. Chem.*, 2024, **138**, 187–199.

59 (*a*) F. Malamiri, S. Khaksar, R. Badri and E. Tahanpesar, *Curr. Org. Synth.*, 2019, **16**, 1185–1190; (*b*) M. R. Asghariganjeh, A. A. Mohammadi, E. Tahanpesar and A. Rayatzadeh, *Mol. Diversity*, 2021, **25**, 509–516; (*c*) A. Zare, E. Jazinizadeh and N. Lotfifar, *J. Appl. Organomet. Chem.*, 2024, **4**(4), 296–309.

60 (*a*) F. Yazdan Kushkoo, H. Khabazzadeh and M. Khaleghi, *Chem. Methodol.*, 2024, **8**(9), 645–661; (*b*) H. Noruzi Moghadam, C. Banaei and A. Bozorgian, *Adv. J. Chem., Sect. B*, 2023, **5**(3), 298–305; (*c*) S. Shahrzad Moayeripour and R. Behzadi, *J. Med. Pharm. Chem. Res.*, 2023, **5**, 303–316.

61 (*a*) L. Sohrabi-Kashani, A. Zolriasatein, B. Eftekhari Yekta and J. Med, *Nanomater. Chem.*, 2023, **2**, 16–32; (*b*) D. Hashim Al-Abboodi and Na. Al-lami, *J. Med. Pharm. Chem. Res.*, 2023, **5**, 343–357; (*c*) Y. Ghalandarzehi and H. Kord-Tamandani, *Asian J. Green Chem.*, 2023, **7**(2), 70–84.

62 (*a*) N. Iravani, B. Karami, F. Asadimoghaddam, M. Monfared and N. Karami, *J. Sulfur Chem.*, 2012, **33**, 279–284; (*b*) M. Keshavarz, N. Iravani, A. Z. Ahmady and M. Vafaei-Nezhad, *J. Chin. Chem. Soc.*, 2015, **62**, 1079–1086; (*c*) H.-L. Yang, L. Zou, A. N. Juaim, C.-X. Ma, M.-Z. Zhu, F. Xu, X.-N. Chen, Y.-Z. Wang and X.-W. Zhou, *Rare Met.*, 2023, **42**, 2007–2019, DOI: 10.1007/s12598-022-02242-4; (*d*) X. Li, H. Zhou, R. Qian, X. Zhang and L. Yu, *Chin. Chem. Lett.*, 2025, **36**, 110036.

63 (*a*) M. M. Al-Tufah, S. Beebaeny, S. Salem Jasim and B. Lateef Mohammed, *Chem. Methodol.*, 2023, **7**, 408–418; (*b*) H. Kefayati, S. Khandan and S. Tavancheh, *Russ. J. Gen. Chem.*, 2015, **85**, 1757–1762; (*c*) E. Ezzatzadeh, M. Mohammadi, Z. S. Hossaini and S. Khandan, *ChemistrySelect*, 2023, **8**(39), e202302491.

64 (*a*) Z. S. Hossaini, M. Mohammadi and F. Sheikholeslami-Farahani, *Front. Chem.*, 2022, **10**, 949205; (*b*) M. M. H. AL-Abayechi, A. Al-nayili and A. A. Balakit, *Inorg. Chem. Commun.*, 2024, **161**, 112076; (*c*) S. S. Moayeripour and R. Behzadi, *J. Med. Pharm. Chem. Res.*, 2023, **5**, 303–316.

65 (*a*) M. Mahmud, M. Jahangir Hossain and J. Med, *Nanomater. Chem.*, 2024, **6**, 208–225; (*b*) M. Kamel, M. Mohammadi, K. Mohammadifard, E. A. Mahmood and M. R. P. Heravi, *Vacuum*, 2023, **207**, 111565; (*c*) M. Anary-Abbasinejada, F. Nezhad-Shshrokhabadi and M. Mohammadi, *Mol. Diversity*, 2019, **24**, 1205–1222.

66 (*a*) T. Kohanfekr, M. Hakimi, H. Hassani and H. Ali Hosseini, *Chem. Methodol.*, 2023, **7**, 748–760; (*b*) E. Israel Edache, A. Uzairu, P. Andrew Mamza and G. Adamu Shallangwa, *Adv. J. Chem., Sect. A*, 2023, **6**(1), 17–30; (*c*) A. Sadeghi Meresht, E. Ezzatzadeh, B. Dehbandi, M. Salimifard and R. Rostamian, *Polycycl. Aromat. Comp.*, 2022, **42**(7), 4793–4808.

67 (*a*) F. Alirezapour, K. Bamdad, A. Khanmohammadi and N. Ebrahimi, *J. Mol. Model.*, 2022, **28**, 302; (*b*) M. N. A. Al-Jibouri, M. A. K. Al-Souz and T. M. Musa, *Asian J. Green Chem.*, 2024, **8**, 247–260; (*c*) F. Hakimi, S. Babaei and E. Golrasan, *Adv. J. Chem., Sect. A*, 2024, **7**, 406–416.

68 (*a*) M. Mubassir, B. R. Parveen, B. Singh, A. Kumar, N. Ahamad and J. Med, *Nanomater. Chem.*, 2024, **6**, 322–334; (*b*) A. Ferdosian, F. Ebadi, M. Z. Mehrabian, R. Golsefidi and M. Varasteh Moradi, *Sci. Rep.*, 2019, 322–334; (*c*) A. Ferdosian, F. Ebadi, M. Z. Mehrabian, R. Golsefidi and M. Varasteh Moradi, *Sci. Rep.*, 2019, 322–334.

69 (*a*) F. Hakimi, S. Babaei and E. Golrasan, *Adv. J. Chem., Sect. A*, 2024, **7**, 406–416; (*b*) E. Ezzatzadeh, M. Mohammadi, M. Ghambarian and Z. S. Hossaini, *Appl. Organomet. Chem.*, 2023, **37**(11), e7252; (*c*) S. Salem Jasim, J. Hilmi Abdulwahid, S. Beebany and B. Lateef Mohammed, *Chem. Methodol.*, 2023, **7**, 509–523.

70 (*a*) S. Soleimani-Amiri, M. Koohi and Z. Azizi, *J. Chin. Biochem. Soc.*, 2018, **65**(12), 1453–1464; (*b*) S. F. Taheri Hatkehlouei, B. Mirza and S. Soleimani-Amiri, *Polycycl. Aromat. Comp.*, 2022, **42**, 1341–1357; (*c*) Y. Cao, S. Soleimani-Amiri, R. Ahmadi, A. Issakhov, A. G. Ebadi and E. Vessally, *RSC Adv.*, 2021, **11**(51), 32513–32525.

71 (*a*) A. Zare, E. Jazinizadeh, N. Lotfifar and J. Appl, *Organomet. Chem.*, 2024, **4**, 296–309; (*b*) Z. S. Hossaini, F. Rostami-Charati, S. Seyfi and M. Ghambarian, *Chin. Chem. Lett.*, 2013, **24**, 376–378; (*c*) M. A. Amiri, H. Younesi,

H. K. Aqmashhadi, G. F. Pasha, S. Asghari and M. Tajbakhsh, *Chem. Methodol.*, 2024, **8**, 1–22.

72 (*a*) R. M. Mhaibes, Z. Arzehgar, M. M. Heydari and L. Fatolahi, *Asian J. Green Chem.*, 2023, **7**, 1–8; (*b*) F. Alirezapour, M. Mohammadi and A. Khanmohammadi, *Chem. Rev. Lett.*, 2023, **6**, 262–275; (*c*) A. R. Ataee-Najari, M. Mohammadi Rasooll, M. Zarei, M. A. Zolfigol, A. Ghorbani Choghamarani and M. Hosseinifard, *RSC Adv.*, 2025, **15**, 10150.

73 (*a*) N. F. Hamedani, F. Z. Hargalani and F. Rostami-Charati, *Mol. Diversity*, 2022, **26**, 2069–2083; (*b*) F. Abed Nashaan and M. Sameer Al-Rawi, *Chem. Methodol.*, 2023, **7**, 267–276; (*c*) S. Rezayati, F. Kalantari and A. Ramazani, *RSC Adv.*, 2023, **13**, 12869.

74 (*a*) E. Davoodi, E. Tahanpesar and A. R. Massah, *ChemistrySelect*, 2021, **6**, 9833–9846; (*b*) K. Khandan-Barani, A. Hassanabadi and M. Abreshteh, *Bulg. Chem. Commun.*, 2019, **51**(4), 475–478; (*c*) N. Karami Hezarcheshmeh and J. Azizianm, *Polycycl. Aromat. Compd.*, 2022, **42**, 7686–7696.

75 (*a*) R. Jalilian, E. Ezzatzadeh and A. Taheri, *J. Environ. Chem. Eng.*, 2021, **9**, 105513; (*b*) F. Adibian, A. R. Pourali, B. Maleki, M. Baghayeri and A. H. Amiri, *Polyhedron*, 2020, **175**, 114179; (*c*) E. Ezzatzadeh, M. Hojjati, A. Parhami and Z. S. Hossaini, *Appl. Organomet. Chem.*, 2024, **38**(12), e7718.

76 (*a*) E. Ezzatzadeh, S. Fallah Lri Sofla, E. Pourghasem, A. Rustaiyan and A. Zarezadeh, *J. Essent. Oil Bear. Plants*, 2014, **17**, 415–421; (*b*) F. Khazaie, S. Shokrollahzadeh, Y. Bide, S. Sheshmani and A. S. Shahvelayati, *Chem. Eng. J.*, 2021, **417**, 129250; (*c*) E. Ezzatzadeh, Z. S. Hossaini, R. Rostamian, S. Vaseghi and S. F. Mousavi, *J. Heterocycl. Chem.*, 2017, **54**, 2909–2911.

77 (*a*) S. Rezayati, F. Kalantari, A. Ramazani and E. Ezzatzadeh, *J. Sulfur Chem.*, 2021, **42**(5), 575–590; (*b*) M. Fattahi, E. Ezzatzadeh, R. Jalilian and A. Taheri, *J. Hazard. Mater.*, 2021, **403**, 123716; (*c*) H. Banary, E. Kolvari and P. Hajiabbasi Tabar Amiri, *J. Appl. Organomet. Chem.*, 2023, **3**, 134–141.

78 (*a*) N. Karami Hezarcheshmeh, F. Godarzbod, N. Faal Hamedanii and S. Vaseghi, *Polycycl. Aromat. Comp.*, 2023, **43**, 9024–9046; (*b*) E. Ezzatzadeh, Z. Hossaini, S. Majedi and F. H. S. Hussain, *Polycycl. Aromat. Comp.*, 2023, **43**, 4707–4728.

79 (*a*) H. B. Farhood, M. N. Radhi and Z. S. Hassan, *J. Med. Nanomater. Chem.*, 2024, **6**, 263–280; (*b*) A. Radhi Obaid and L. Shiri, *J. Appl. Organomet. Chem.*, 2024, **4**, 178–189.

80 (*a*) S. A. Nirwan, S. A. Shinde, R. A. Ughade, V. B. Tadke and S. A. Dhanmane, *Asian J. Green Chem.*, 2025, **9**, 291–309; (*b*) K. Khandan-Barani, M. Kangani, M. Mirbaluchzehi and Z. Siroos, *Inorg. Nano-Met. Chem.*, 2017, **47**, 751–755; (*c*) M. Farajpour, S. M. Vahdat, S. M. Baghbanian and M. Hatami, *Chem. Methodol.*, 2023, **7**(7), 540–551.

81 K. Shimada, K. Fujikawa, K. Yahara and T. Nakamura, *J. Agric. Food Chem.*, 1992, **40**, 945–948.

82 G. C. Yen and P. D. Duh, *J. Agric. Food Chem.*, 1994, **42**, 629–632.

83 A. Yildirim, A. Mavi and A. A. Kara, *J. Agric. Food Chem.*, 2001, **49**, 4083–4089.

84 A. Chanda and V. V. Fokin, *Chem. Rev.*, 2009, **109**(2), 725–748.

85 S. Narayan, J. Muldoon, M. G. Finn, V. V. Fokin, H. C. Kolb and K. Barry Sharpless, *Angew. Chem., Int. Ed.*, 2005, **44**(21), 3275–3279.

86 R. N. Butler and A. G. Coyne, *Org. Biomol. Chem.*, 2016, **14**, 9945–9960.

87 M. M. Moghadam and M. Zamani, *Comput. Theor. Chem.*, 2021, **1198**, 113185.

88 M. M. Moghadam and M. Zamani, *Int. J. Quantum Chem.*, 2021, **121**, e26504.

89 S. Sarvarian and M. Zamani, *Struct. Chem.*, 2021, **32**, 1205–1217.

90 A. R. Saundane and M. K. Nandibeoor, *Monatsh. Chem.*, 2015, **146**, 1751–1761.

91 A. M. Bidchol, A. Wilfred, P. Abhijna and R. Harish, *Food Bioprocess Technol.*, 2011, **4**, 1137–1143.